processes

MDPI

*Article*

# Immobilization of Laccase on Hybrid Super-Structured Nanomaterials for the Decolorization of Phenolic Dyes

**Michaela Patila [1,*], Panagiotis E. Athanasiou [1], Lampros Kortessis [1], Georgia Potsi [2], Antonios Kouloumpis [2], Dimitrios Gournis [2] and Haralambos Stamatis [1,*]**

[1] Biotechnology Laboratory, Department of Biological Applications and Technology, University of Ioannina, 45110 Ioannina, Greece; p.athanasiou@uoi.gr (P.E.A.); bbrosla187@gmail.com (L.K.)
[2] Department of Materials Science and Engineering, University of Ioannina, 45110 Ioannina, Greece; gepotsi@gmail.com (G.P.); antoniokoul@gmail.com (A.K.); dgourni@uoi.gr (D.G.)
* Correspondence: pstm10345@uoi.gr (M.P.); hstamati@uoi.gr (H.S.)

**Abstract:** In the present work, hybrid super-structured nanomaterials were synthesized by the combination of smectite nanoclays with various carbon-based nanomaterials (graphene oxide, carbon nanotubes and adamantylamine) and were used as nanosupports for the covalent and non-covalent immobilization of laccase from *Trametes versicolor* (TvL). TvL was successfully immobilized on these hybrid nanomaterials, achieving high immobilization yields (up to 85%), while its conformation remained unaltered upon immobilization. The apparent kinetic constants $V_{max}$ and $K_m$ of the immobilized enzymes strongly depended on the immobilization procedure and the composition of hybrid nanomaterials. Immobilized TvL preserved up to 50% of its initial activity after 24 h of incubation at 60 °C, while free enzyme was totally deactivated. The TvL-hybrid nanomaterials bioconjugates were efficiently applied for the degradation of various synthetic dyes, exhibiting excellent decolorization capacity, as well as high reusability (up to 11 successive catalytic cycles), providing insights into the use of these bionanoconjugates on applications with environmental, and industrial interest.

**Keywords:** dye decolorization; hybrid nanomaterials; laccase; immobilization; green bioprocesses



**Citation:** Patila, M.; Athanasiou, P.E.; Kortessis, L.; Potsi, G.; Kouloumpis, A.; Gournis, D.; Stamatis, H. Immobilization of Laccase on Hybrid Super-Structured Nanomaterials for the Decolorization of Phenolic Dyes. *Processes* **2022**, *10*, 233. https://doi.org/10.3390/pr10020233

Academic Editors: Lai-Chang Zhang, Shun-Xing Liang and Zhe Jia

Received: 24 December 2021
Accepted: 20 January 2022
Published: 26 January 2022



## 1. Introduction

Dyes are chemical compounds that are used extensively in textile and printing industry [1,2]. Dye decomposition results in the production of several toxic substances which are released in the environment through waste effluents, causing toxic, mutagenic or carcinogenic problems [3,4]. Thus, dye degradation or modification of the produced by-products is of critical significance. So far, the elimination of dyes is performed by a variety of methods, including chemical oxidation, adsorption, co-precipitation or photodegradation [4]. However, the application of such physicochemical approaches displays some major disadvantages, such as application of high-cost and complicated operations, use of large amount of chemicals, production of more toxic by-products, and generation of toxic sludge that leads to secondary pollution [5,6]. An alternative and environmental-friendly procedure relies on enzymatic treatment, as the products of enzymatic degradation are less toxic than the pristine synthetic dyes and they can be utilized by different natural organisms [7,8]. Additionally, enzymatic treatment can occur at a wide range of pH and temperature, and against high concentrations of pollutants [9]. Fungal and microbial laccases have been widely explored towards their use in textile water treatment for dye decolorization and detoxification, via degradation or polymerization reactions, due to their oxidation power and ability to oxidize different chemical compounds [10]. Laccases (benzendiol:oxygen oxidoreductases, EC 1.10.3.2) are multi-copper containing oxidases, that catalyze the one-electron oxidation of a wide range of organic and inorganic substances, through the reduction of molecular oxygen to water [11,12]. Laccases exhibit

broad substrate specificity, thus they are widely applied in wood fiber modification, chemical or medicinal synthesis, detoxification of pollutants, and biological bleaching in pulp and paper industries [13–15].

However, the use of enzymes in industrial scale is limited due to some main drawbacks they present, such as high solubility, low stability under conditions of high temperatures, extreme pH values or use of organic co-solvents, and incapability of being used for successive reaction cycles [16]. Immobilization of enzymes on supports provides a solution to this problem. Amongst the supports used to date, carbon-based nanomaterials, such as graphene oxide and carbon nanotubes, as well as their composites, find application in different fields, for instance in sensing, bio-imaging, energy storage and catalysis [17–20], while they are also promising candidates as immobilization carriers. Due to their unique characteristics such as biocompatibility, excellent chemical, mechanical and thermal stability, large surface area and ability of easy surface modification by diverse functional groups, these nanomaterials are able to interact with protein molecules, leading to high protein loading and to the development of robust nanobiocatalysts with improved biocatalytic and structural characteristics [16].

Herein, we report the synthesis of hybrid super-structures, based on the combination of smectite clays with different carbon-based nanomaterials, and their application as nanosupports for the immobilization of laccase from *Trametes versicolor* (TvL). The combination of relevant and desirable features of different materials may result in the synthesis of hybrid or composite materials that present a broad spectrum of properties, e.g., enhanced mechanical properties, dimensional stability, thermal and chemical stability, and electrical conductivity [21]. Smectite clays are 2D layered minerals with sheet-like geometry, consisted of aluminosilicate nanoplatelets, where each layer is composed by a combination of an octahedral and a tetrahedral sheet. They present excellent properties such as cation exchange capacity, porosity, swelling response and intercalation capacity [21,22], which make them valuable nanostructures for applications in catalysis, organic synthesis, and adsorption of inorganic/organic components, such as pollutants and dyes [21,23–25]. The nature of the organized structure between the aluminosilicate sheets, as well as their tailor-made properties using simple techniques, may result in the controlled intercalation of molecules, and thus making them versatile supports for the specific immobilization of a plethora of biomolecules, such as enzymes [26]. The chemical and structural properties of layered smectite clays could be tailored and further improved by the addition of organic or polymeric molecules [27]. Graphene oxide (GO), oxidized multi-walled carbon nanotubes (CNTs) and adamantylamine (ADA) were chosen as the organic components for the synthesis of the hybrid super-structured nanomaterials. GO is a 2D carbon nanomaterial owing to excellent chemical reactivity, thermal and mechanical stability, and is widely applied in the development of biosensors, drug delivery, and enzyme immobilization [17,18]. CNTs, consisting of a concentric cylindrically order of graphene sheets, are also being explored for a wide range of biological applications, due to their structure and mechanical properties [28,29]. Adamantylamime (ADA), the amine-derivative of the smallest nanodiamond, adamantane, is widely applied in pharmaceutical industry due to its low toxicity [25]. Moreover, ADA is used in nanotechnology for nanomaterial functionalization, due to its unique structure of tricyclic saturated hydrocarbons [25]. For instance, it has been reported that when ADA is intercalated between clay and/or GO sheets, it provides the resulted nanocomposites with a greater interlayer space, increasing their capacity in phenolic derivatives adsorption, e.g., chlorophenols, compared to the parental materials [25]. This characteristic makes ADA a promising candidate for nanomaterial functionalization towards their use in adsorption of phenolic pollutants.

In the present work, the synthesized hybrid nanomaterials, namely Clay-ADA, Clay-CNTs and Clay-GO, were used as supports for both covalent and non-covalent immobilization of laccase. The novel nanobiocatalysts that were designed were studied for their biocatalytic activity, by determining their apparent kinetic parameters, while Fourier-transform infrared (FTIR) spectroscopy was used to investigate the effect of the hybrid

nanomaterials on the structure of TvL. Finally, the prepared immobilized biocatalysts were applied for the decolorization of various synthetic dyes, providing insights into the use of immobilized enzymes in applications of biotechnological, environmental, and industrial interest.

## 2. Materials and Methods

### *2.1. Materials*

Laccase from *Trametes versicolor* (13.6 U $mg^{-1}$, TvL), 2,2′-azino-bis(3-ethylbenzothiazoline-6-sulphonic acid) (ABTS), methyl orange, bromophenol blue, bromothymol blue, phenol red, Coomassie brilliant blue G250, 1-hydroxybenzotriazole (HBT), *N*-hydroxysuccinimide (NHS), 1-ethyl-3-(3-dimethylaminopropyl) carbodiimide hydrochloride (EDC) and 2-[4-(2-hydroxyethyl)piperazin-1-yl]ethanesulfonic acid (HEPES) were obtained from Sigma (St. Louis, MO, USA). Glutaraldehyde solution 25% was purchased from Merck (KGaA, Darmstadt, Germany). All other reagents were of analytical grade.

### *2.2. Synthesis of Hybrid Nanomaterials*

The synthesis and characterization of the hybrid nanostructures have been previously published [25,30]. For this reason, a short description of the experimental details regarding the synthetic protocols of the nanomaterials is presented in this work, while the extended details can be found in the respected references.

For the synthesis of Clay-ADA, 300 mg of sodium clay (SWy-2, Source Clay Minerals Repository, University of Missouri, Columbia, MO, USA) were dispersed in 100 mL $H_2O$ and then reacted with 100 mL of a 20:1 (*v*/*v*) ethanol: water solution containing 50 mg of 1-adamantylamine (97%, Aldrich, St. Louis, MO, USA). Five drops of a 1 M aqueous solution HCl were added and the mixture was stirred for 24 h [25], followed by centrifugation (3500 rpm, 30 min), washed three times with $H_2O$ and air-dried.

For the synthesis of Clay-CNTs, 500 mg of sodium clay (Zenith, S&B Industrial minerals S.A., Milos, Greece) were dispersed in 100 mL $H_2O$ and reacted with 100 mL of a 0.01 M aqueous solution of $NiCl_2 \cdot 6H_2O$ and $FeCl_2 \cdot 6H_2O$ for 3 h, to obtain Ni/Fe-exchanged clay [31–33]. The clay was separated by centrifugation (3500 rpm, 30 min), rinsed with $H_2O$, air-dried and calcinated at 450 °C for 4.5 h. Next, 100 mg of the Ni/Fe-clay were placed in an alumina boat, inserted in a tubular furnace (inner diameter of 2.2 cm and length of 90 cm), heated up to 700 °C under an argon (Ar) atmosphere and reacted with acetylene for 30 min, using a feed flow of argon/acetylene mixture (10 and 90 $cm^3$ $min^{-1}$, respectively). Lastly, the resulted hybrid was oxidized by dispersion in a solution of 60 mL $H_2SO_4$ and 20 mL $HNO_3$ (3:1 (*v*/*v*)) followed by sonication for 3 h. The final hybrid residue was dispersed in $H_2O$, centrifuged (3500 rpm, 30 min), washed with $H_2O$ and air-dried.

For the synthesis of Clay-GO, 100 mg of sodium montmorillonite (SWy-2) and 100 mg of GO, produced by a modified Staudenmaier's method from graphite powder [34,35], were separately dispersed in 500 mL of $H_2O$ and stirred overnight. Next, the two dispersions were mixed and let under vigorous stirring for additional 18 h. The final hybrid was centrifuged (3500 rpm, 30 min) and air-dried [36].

The structure of the synthesized nanomaterials is depicted in Scheme 1.

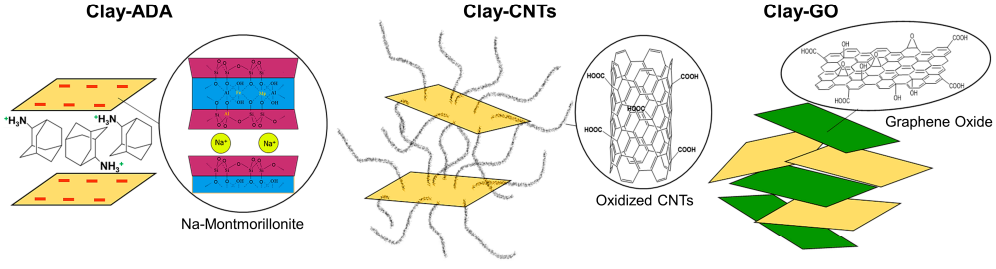


**Scheme 1.** Structure of the hybrid super-structured nanomaterials.

### 2.3. Non-Covalent Immobilization of TvL

3 mg of the hybrid nanomaterials were dispersed in 5 mL of acetate buffer (0.1 M, pH 4.58) and left in an ultrasonic bath for 30 min. In the next step, 1 mL of TvL solution (containing 3 mg TvL) was added in the nanomaterial dispersion and the mixture was incubated for 1 h under stirring (300 rpm), at 30 °C. The hybrid nanomaterial-TvL bioconjugates were separated by centrifugation at 6000 rpm for 10 min and washed thrice with 1 mL buffer solution to remove any loosely bound protein. The biocatalysts were dried over silica gel and stored at 4 °C until used.

### 2.4. Covalent Immobilization of TvL Using Glutaraldehyde as Cross-Linker

3 mg of hybrid nanomaterials with free amine groups (such as Clay-ADA) were dispersed in 9.13 mL of acetate buffer (0.1 M, pH 4.58) and left in an ultrasonic bath for 30 min, in the presence of 110 μL Tween-20. As a next step, 1.76 mL of a glutaraldehyde solution 25% was added and the mixture was incubated for 1 h under stirring (300 rpm) at 30 °C. The modified hybrid nanomaterials were separated from the mixture by centrifugation at 6000 rpm for 10 min and washed thrice with 2 mL buffer solution to remove the excess of glutaraldehyde. The activated hybrid nanomaterials were re-dispersed in 5 mL of acetate buffer. Then, 1 mL of protein solution in acetate buffer (containing 3 mg TvL) was added, and the steps described for non-covalent procedure were followed.

### 2.5. Covalent Immobilization of TvL via Diimide-Activated Amidation

3 mg of hybrid nanomaterials with free carboxyl groups (such as Clay-CNTs and Clay-GO) were dispersed in 5 mL distilled water and left in an ultrasonic bath for 30 min. In the following step, 1.2 mL of a 10 mg $mL^{-1}$ EDC aqueous solution and 2.3 mL of a 50 mg $mL^{-1}$ NHS aqueous solution were added to the above suspension, and the mixture was incubated for 30 min under stirring (300 rpm) at 30 °C. The activated hybrid nanomaterials were separated from the mixture by centrifugation at 6000 rpm for 10 min and washed thrice with 2 mL distilled water to remove the excess of EDC/NHS. The activated hybrid nanomaterials were re-dispersed in 5 mL of HEPES buffer solution (0.1 M, pH 4.58). Then, 1 mL of protein solution in HEPES buffer (containing 3 mg TvL) was added, and the steps described for non-covalent procedure were followed.

### 2.6. Immobilization Efficiency

The amount of immobilized enzyme was calculated by measuring the protein concentration existing in the supernatant after the immobilization procedure, using the Bradford assay [37]. Enzyme loading was determined as the difference between the concentration of the protein in the supernatant after immobilization and the initial concentration of the protein.

### 2.7. Fourier-Transform Infrared Spectroscopy

Fourier-transform infrared spectroscopy (FTIR) was used to examine alterations in the conformation of immobilized TvL on hybrid nanomaterials. The spectra were recorded in the range of 400–4000 $cm^{-1}$, using a FTIR-8400 infrared spectrometer (Shimadzu, Tokyo, Japan) equipped with a deuterated triglycine sulfate (DTGS) detector. For each sample, a total of 64 scans were averaged, using a 4 $cm^{-1}$ resolution. The samples were prepared as KBr pellets containing a circa 1 wt% sample. The similarity of FTIR spectra in the Amide I region (1600–1700 $cm^{-1}$) was evaluated by estimation of the correlation coefficient, $r$, using the following equation:

$$r = \frac{\Sigma xiyi}{\sqrt{\Sigma xi^2 \Sigma yi^2}} \quad (1)$$

where $x$ and $y$ describe the spectral absorbance values of the reference (free enzyme) and sample (immobilized enzyme) spectra, respectively, at the $i$th frequency position [38,39]. For identical spectra, the $r$ value is equal to 1.0, while spectra differences are depicted as decreased $r$ values.

### 2.8. Determination of Apparent Kinetic Constants

Laccase activity was determined by ABTS oxidation at room temperature [40]. For the determination of the apparent kinetic constants $V_{max}$ and $K_m$ of free and immobilized laccase, proper volumes of TvL and buffer solution (0.1 M, pH 4.58) were mixed and then ABTS was added to a final concentration range of 0.01–2.0 mM. The oxidation of ABTS was detected at 415 nm ($\varepsilon_{ABTS+}$ = 36,000 $M^{-1}$ $cm^{-1}$) using a UV-visible spectrophotometer (Shimadzu, Tokyo, Japan). The apparent kinetic parameters were calculated using non-linear regression analysis (EnzFitter, Biosoft, UK). All experiments were carried out in triplicate. One unit was defined as the amount of the enzyme that oxidizes 1 μmol of ABTS per min.

### 2.9. Stability of TvL

Free or immobilized TvL was incubated in acetate buffer (0.1 M, pH 4.58) for up to 24 h at 60 °C. Samples were taken at specific time periods to determine the remaining activity of the enzyme, through the ABTS oxidation, as described above.

### 2.10. Dye Decolorization by TvL

The decolorization of the dyes was carried out in a mixture of 1.5 mL, consisting of 37.5–150 μM dye, 0.1 M acetate buffer (pH 4.58), 1 mM HBT and 0.1 mg of immobilized enzyme. The reaction mixtures were incubated in a rotary shaker (120 rpm) at 30 °C, for up to 48 h. Samples (0.2 mL) were taken from each reaction mixture in specific time intervals, transferred to a 98-well microplate, and the decrease in the maximum absorbance of the dyes was recorded (450 nm for bromothymol blue, methyl orange and phenol red; 545 nm for bromophenol blue and Coomassie brilliant blue). Dye decolorization was calculated by the formula:

$$\text{Decolorization (\%)} = [(A_i - A_t)/A_i] \times 100, \quad (2)$$

where $A_i$: initial absorbance of the dye at $t$ = 0, $A_t$: absorbance of the dye at each time interval. Each decolorization experiment was performed in triplicate and the mean of decolorization (%) was reported.

### 2.11. Reusability of Immobilized TvL

The reusability of the immobilized TvL on hybrid nanomaterials was investigated for the decolorization of methyl orange, performed in a handmade enzyme-immobilized microreactor consisting of a glass tube with an inner diameter of 0.9 mm and a length of 40 mm, and packed with 1.1 mg immobilized TvL. In each catalytic cycle, the mixture (containing 75 μM dye and 1 mM HBT) was pumped through the continuous microreactor at 30 °C, with 2 mL $h^{-1}$ pumping flow rate. The decolorization efficiency was defined as described previously, by measuring the absorbance before and after the entrance in the microreactor.

## 3. Results and Discussion

### 3.1. Immobilization of TvL on Hybrid Nanomaterials

In the present work, TvL was immobilized on hybrid super-structured nanomaterials to develop robust nanobiocatalysts. Immobilization of TvL was carried out via covalent binding and physical adsorption, and the immobilization yields are presented in Table 1. It is worthy to mention that the chosen immobilization conditions were the result of a preliminary optimization study. As seen from Table 1, TvL was successfully immobilized on all hybrid nanomaterials, regardless the immobilization procedure that was followed. In some cases, the immobilization yield was higher compared to previously reported works for immobilized laccase on different nanosupports [41,42]. The high immobilization yields could be attributed to the improved properties these hybrid nanomaterials exhibit, such as high surface area and mechanical stability. Comparing the two immobilization methods, laccase was more efficiently immobilized through physical adsorption rather that covalent

binding. This may be a result of the limited number of free functional groups existing on the surface of the nanomaterials and are available for covalent bonding, restricting the specific enzyme attachment [43].

**Table 1.** Immobilization yield (%) of TvL on hybrid nanomaterials.

| Nanomaterial | Immobilization Yield (%) [1] | |
|---|---|---|
| | Non-Covalent | Covalent |
| Clay-ADA | 80 ± 1.8 | 73 ± 2.1 |
| Clay-CNTs | 71 ± 0.8 | 69 ± 1.1 |
| Clay-GO | 85 ± 1.1 | 72 ± 0.8 |

[1] Calculated as the ratio of protein immobilized on nanomaterials to the initial protein amount.

Regarding non-covalent immobilization, TvL is adsorbed on the hybrid nanostructures through the development of different kind of interactions, mainly by electrostatic, hydrophobic, π-π interactions, or by a combination of them. For instance, in the case of Clay-ADA, electrostatic interactions developed between the positively charged nanomaterial (due to the presence of the amine group in ADA) and the negatively charged enzyme (pI 2.8–4.0), may be the driving forces during the immobilization procedure. On the other hand, both Clay-CNTs and Clay-GO are negatively charged, due to the presence of carboxylic groups on the carbon-based component, thus the adsorption is driven mainly by hydrophobic and π-π interactions with the basal planes of the nanomaterials. The highest immobilization yield was observed when Clay-GO was used as support. This hybrid nanomaterial combines the properties of both GO and clay, which belong to the category of 2D layered materials and have a large surface area and a large aspect ratio [25]. The combination of these two nanomaterials enhances the surface area of the resulted hybrid composite [25], leading to strong interactions with TvL, and thus promoting the loading of the enzyme [38,44]. This is in accordance with that observed for the immobilization of proteins on composite materials containing montmorillonite [45].

### *3.2. Structural Studies of Immobilized TvL on Hybrid Nanomaterials by FTIR*

Into the interest of evaluating the structural changes of TvL upon immobilization on hybrid nanomaterials, FTIR spectroscopy was applied, as this method does not suffer from light scattering perturbations, and thus can be used for conformational studies of a protein immobilized on a solid support. The FTIR spectra are presented in Figure S1, where the Amide I and Amide II bands, corresponding to stretching vibrations of the polypeptide backbone of the protein, can be observed at the regions 1630–1640 and 1540–1560 $cm^{-1}$, respectively [43]. By manipulating the data from the IR spectra, the correlation coefficient *r* was calculated in the Amide I region (1600–1700 $cm^{-1}$), according to previously published work [38,39,46], and the results are presented in Table 2. As seen, the *r* values of immobilized TvL were close to 1.0, indicating that the enzyme preserved its native secondary structure after immobilization. A slight decrease of the *r* coefficient value was observed when Clay-CNTs were used as immobilization support. This decrease could render from slight conformational changes during TvL immobilization on the nanosupport. It has been proposed that during enzyme immobilization on clay minerals, only some side chains of the enzyme molecule intercalate within the nanosheets, while the biggest part of the polypeptide chain is localized outside the main structure [26].

**Table 2.** Correlation coefficient (*r*) of immobilized TvL on hybrid nanomaterials.

| Enzyme | *r* | |
|---|---|---|
| | Non Covalent | Covalent |
| Clay-ADA | 0.996 | 0.986 |
| Clay-CNTs | 0.986 | 0.983 |
| Clay-GO | 0.993 | 0.990 |

### 3.3. Kinetic Studies of TvL

The apparent kinetic constants $V_{max}$ and $K_m$ of the immobilized laccase on hybrid nanomaterials were determined by using ABTS (0.01–2.0 mM) as substrate. The results of the kinetic analysis indicated that a Michaelis–Menten mechanism occurs in the system. It can be observed from Table 3 that regardless the immobilization procedure and the nature of the nanosupports, the apparent $V_{max}$ value decreased in the case of immobilized TvL, leading to a reduction of the catalytic efficiency, with respect to free enzyme. This result indicated limited conformational changes in the enzyme molecule after immobilization [47] or limited approachability of the substrate to the active site of TvL [42]. Similar decrease of the $V_{max}$ value has been reported for immobilized TvL on amine-functionalized $Fe_3O_4$@C nanoparticles [48]. The highest apparent $V_{max}$ value was observed when Clay-GO was used as immobilization carrier, a finding in agreement with the structural preservation of TvL after immobilization on this nanomaterial, indicating that the nature of the carbon component of the hybrid nanomaterials plays an important role; the presence of GO and CNTs on the clay structure enhances the activity of the enzyme, while the lowest catalytic ability was observed in the case of ADA.

**Table 3.** Determination of the apparent kinetic parameters of free and immobilized TvL.

| Enzyme | $V_{max}$ (μM/min*μg Immobilized Enzyme) | $K_m$ (mM) |
|---|---|---|
| Free TvL | 9.31 ± 0.06 | 0.13 ± 0.01 |
| Non-covalent | | |
| Clay-ADA | 0.20 ± 0.04 | 0.15 ± 0.02 |
| Clay-CNTs | 0.32 ± 0.10 | 0.12 ± 0.02 |
| Clay-GO | 0.37 ± 0.03 | 0.10 ± 0.01 |
| Covalent | | |
| Clay-ADA | 0.23 ± 0.04 | 0.06 ± 0.01 |
| Clay-CNTs | 1.62 ± 0.08 | 0.15 ± 0.01 |
| Clay-GO | 2.39 ± 0.20 | 0.09 ± 0.03 |

$K_m$ value is a useful tool in probing the ability of an enzyme to bind to its substrate. The apparent $K_m$ value of free TvL was calculated at 0.13 mM, while the apparent $K_m$ values of immobilized TvL depended on the nature of the nanosupport and ranged from 0.06 to 0.15 mM. In most cases, a decrease in apparent $K_m$ values was observed for immobilized laccase. In the cases of non-covalently and covalently immobilized TvL on Clay-ADA and Clay-CNTs, respectively, the apparent $K_m$ values were higher than that of the free enzyme, a result that indicated a lower enzyme-substrate complex formation, probably due to changes in enzyme's structure during the immobilization procedure, loss of enzyme flexibility that is crucial for appropriate substrate binding, or steric hindrance and diffusion limitations due to smectite particles, as evidenced in previous works for immobilized enzymes on clay/chitosan hybrid nanomaterials [27,49,50].

### 3.4. Stability of TvL

The stability of free and immobilized TvL on the hybrid nanomaterials was investigated after incubation at 60 °C in acetate buffer (0.1 M, pH 4.58). As seen in Figure 1, free TvL lost ~90% of its initial activity after 1 h incubation at 60 °C, while after 24 h the enzyme was totally deactivated. On the other hand, the immobilization of TvL on hybrid nanomaterials resulted in enzyme stabilization, regardless the immobilization procedure that was followed. For instance, non-covalently immobilized TvL on Clay-CNTs preserved 50% of its initial activity after 24 h incubation. The results indicated that these hybrid nanomaterials offer a protective environment for TvL, resulting in higher stability against denaturing conditions, such as high temperature. The immobilization procedure enhances the inflexibility of the enzyme by stabilizing its 3D structure, and making it less exposed to harsh conditions [51]. The reduced molecular mobility of the enzyme and a possible improved conformational stabilization, due to the formation of stable covalent bonds between

the hybrid nanomaterials and TvL, results in enhanced stabilization of the enzyme against thermal denaturation [52]. The effect of other carbon-based nanomaterials as supports for enzyme stabilization has been already reported by our team [52,53] and is in accordance with the results presented in this work. The stabilizing effect depended on the kind of nanomaterial. For instance, non-covalently immobilized TvL on Clay-CNTs and Clay-GO, and covalently immobilized TvL on Clay-ADA exhibited higher thermal stability even after 24 h incubation (50, 40 and 32%, respectively) compared to the other biocatalysts, while their catalytic activity was found to be reduced (Table 3), indicating that the immobilization of TvL on these nanomaterials results in less active but more stable biocatalysts.

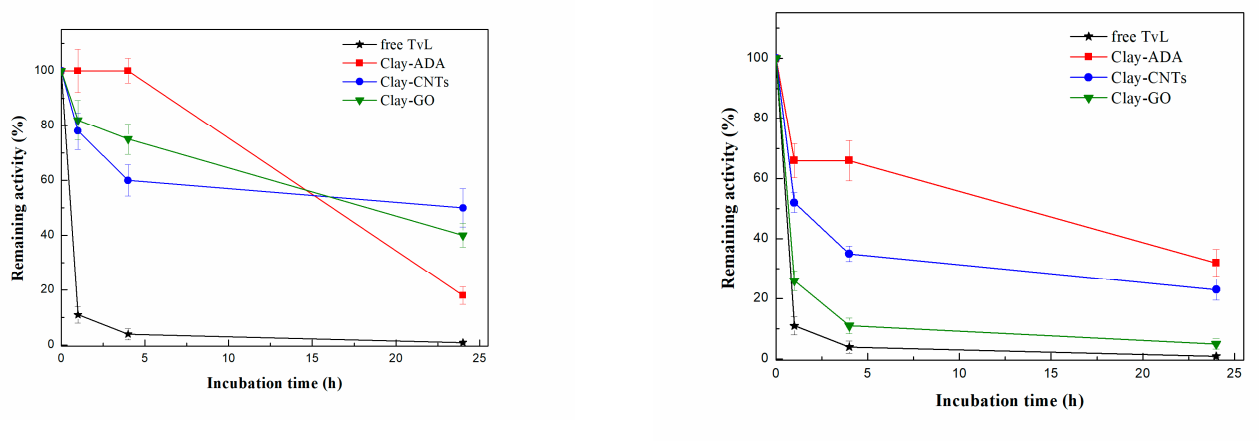


**Figure 1.** Stability of (**a**) non-covalently and (**b**) covalently immobilized TvL on hybrid nanomaterials, after incubation in acetate buffer, at 60 °C. As 100% is indicated the enzyme activity at t = 0.

### *3.5. Use of Immobilized TvL for Decolorization of Dyes*

The dye-decolorizing potential of immobilized TvL on hybrid nanomaterials was demonstrated for five different synthetic dyes: bromophenol blue, bromothymol blue, Coomassie brilliant blue, methyl orange and phenol red. These phenolic compounds belong to different dye families, based on their chemical structures, namely sulphur, triphenylmethane and azo dyes, which are found in most textile effluents [54]. The results are presented in Table 4 and Figure S2. The presence of HBT was necessary to decolorize the synthetic dyes, since no decolorization was detected in its absence, a result which has been previously reported for laccase immobilized on CNTs [55]. HBT acted as mediator, extending the oxidation of non-specific substrates by TvL. In most cases, immobilized TvL was able to efficiently catalyze the decolorization of the dyes. The decolorization could be attributed to the combined effects of enzymatic degradation by immobilized TvL and the sorption capacity of the hybrid nanosupports [56]. The clay components of the hybrid nanomaterials are known to act as adsorbents for organic compounds and pollutants, such as phenolic compounds and synthetic dyes [25]. It seems that the sorption capacity of these clay-based nanomaterials may attract dye molecules to their surface and/or pores, and thereby transfer them in close vicinity to the active center of TvL, enhancing the enzymatic decolorization.

The decolorization efficiency of the immobilized TvL depended on both the immobilization carrier and the immobilization procedure. The decolorization yields of covalently immobilized TvL on hybrid nanomaterials were significantly higher compared to non-covalently immobilized TvL, which is associated with the increased catalytic activity of covalently immobilized enzyme described in Table 3. Immobilized TvL on Clay-CNTs was found to exhibit the highest decolorization yields against most of the dyes. This result is in accordance with the high catalytic activity observed for immobilized TvL on this nanomaterial. Immobilized TvL on Clay-GO was also found to exhibit high decolorization yields, while immobilized TvL on Clay-ADA presented the lowest decolorization capacity,

indicating that the nature of the carbon component of the hybrid nanomaterials plays a critical role for the effectiveness of the resulting nanobiocatalyst. This observation may arise from the different porous size of the hybrid nanomaterials [25]. ADA is a small molecule, compared to CNTs and GO, so when it is intercalated in the clay sheets, the inner space is smaller compared to that achieved when CNTs and GO are intercalated in the clay structure, and thus resulting in a lower adsorbing capacity of the nanomaterial, as previously discussed. In most cases, the nanobiocatalysts that were used in the present work exhibited higher decolorization capacity than that reported for the decolorization of textile dyes by immobilized laccase on calcium alginate beads [57] or for the decolorization of bromophenol blue by immobilized laccase on copper alginate bead [58], indicating that these hybrid super-structures can be effectively used as supports for the development of robust nanobiocatalysts with high potential in dye removal applications.

**Table 4.** Decolorization of different dyes by immobilized TvL on hybrid nanomaterials.

| Enzyme | Decolorization (%) [1] | | | | |
|---|---|---|---|---|---|
| | **Bromophenol Blue (48 h)** | **Bromothymol Blue (48 h)** | **Coomassie Brilliant Blue (48 h)** | **Methyl Orange (48 h)** | **Phenol Red (48 h)** |
| Non-covalent | | | | | |
| Clay-ADA | 5 ± 0.7 | 43 ± 0.2 | 40 ± 8.0 | 18 ± 1.4 | 11 ± 5.0 |
| Clay-CNTs | 19 ± 4.8 | 66 ± 2.0 | 45 ± 6.0 | 38 ± 2.4 | 50 ± 7.1 |
| Clay-GO | 10 ± 1.1 | 65 ± 0.9 | 33 ± 1.6 | 23 ± 1.0 | 15 ± 4.1 |
| Covalent | | | | | |
| Clay-ADA | 24 ± 1.0 | 71 ± 1.4 | 61 ± 3.8 | 60 ± 1.9 | 25 ± 6.7 |
| Clay-CNTs | 85 ± 3.7 | 74 ± 2.4 | 91 ± 1.9 | 87 ± 1.2 | 67 ± 7.8 |
| Clay-GO | 70 ± 9.0 | 75 ± 1.3 | 91 ± 4.1 | 89 ± 2.0 | 80 ± 1.4 |

[1] The reaction was conducted in acetate buffer (0.1 M, pH 4.58), at 30 °C.

The highest decolorization yield for both non-covalently and covalently immobilized TvL was observed when bromothymol blue was used as substrate. Figure 2 shows the full decolorization profile of bromothymol blue against time. It can be observed that immobilized TvL was able to catalyze up to 70% decolorization of bromothymol blue even after 4 h. This decolorization capacity is similar to that observed for immobilized laccase in alginate-gelatin mixed gel [59] and higher than that reported for crude laccase from *Aspergillus niger* [60].

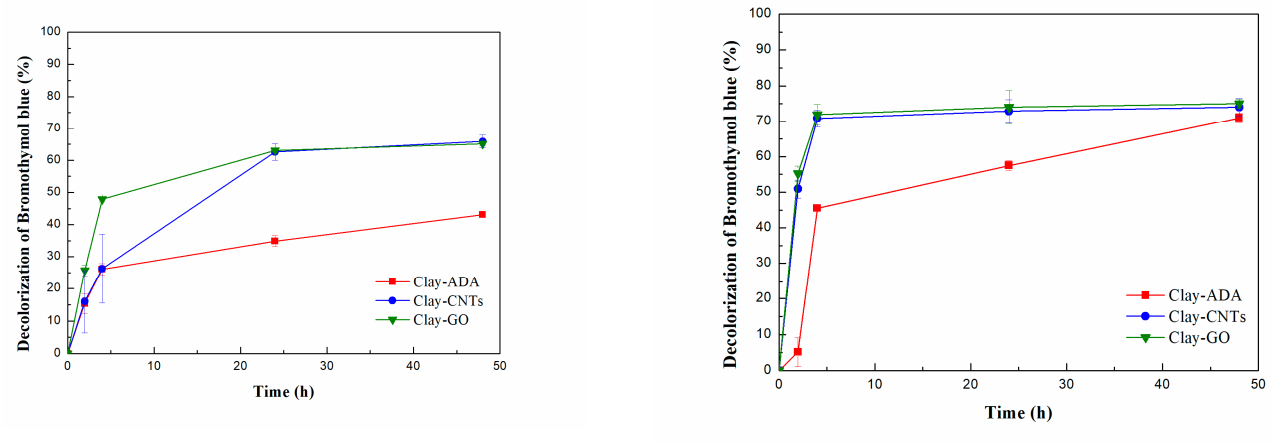


**Figure 2.** Decolorization yield (%) of bromothymol blue by (**a**) non-covalently and (**b**) covalently immobilized TvL on hybrid nanomaterials.

As dyes are found in various concentrations in the environment, immobilized TvL was further used to investigate its capability of decolorizing different dye concentrations. For this reason, covalently immobilized TvL on Clay-CNTs and Clay-GO were selected for the next experiments, as these nanobiocatlaysts exhibited the highest decolorization yields. The results are presented in Figure S3. As it can be seen, the initial dye concentration affected the catalytic activity of the immobilized enzymes. More specifically, both nanobiocatalysts exhibited low decolorization capability when the initial concentration of the dyes was 37.5 μM. When the concentration of the dye raised at 75 μM, immobilized TvL reached decolorization yields up to 91%, depending on the substrate. Further increase of dye concentration in the reaction mixture resulted in decrease of the decolorization yield. This reduction in the efficiency of the biocatalysts probably renders from the structural complicity of these dyes, preventing complete removal from the reaction mixtures of high dye concentrations. This result is in accordance to that previously reported for laccase immobilized on $TiO_2$-$ZrO_2$ and $TiO_2$-$ZrO_2$-$SiO_2$ nanomaterials and its use for dye degradation [61].

### *3.6. Reusability of Immobilized TvL*

An important advantage of the use of immobilized enzymes in industrial biocatalytic processes is their ability to be recovered and reused, and thus decreasing the cost of production. Hence, the decolorization of methyl orange by covalently immobilized TvL on Clay-CNTs and Clay-GO was studied as a model biocatalytic process through successive cycles. The reusability experiments took place in an enzyme-immobilized microreactor at a 2 mL $h^{-1}$ pumping flow rate. Enzyme-immobilized microreactors are being explored and applied in chemistry and biotechnology fields, as they offer a variety of advantages, such as rapid heat exchange and mass transfer, large surface and interface area, and formation of laminar flow of the streams, which allow strict control of the reaction conditions [62,63].

The results of the reusability of covalently immobilized TvL on Clay-CNTs and Clay-GO are presented in Figure 3. The synthesized nanobiocatalysts kept a significant part of their decolorization capacity even after 11 repeated cycles (48 h of total operation time at 30 °C). Immobilized TvL on Clay-CNTs and Clay-GO was able to catalyze the decolorization of methyl orange, with decolorization yields of 56.5 and 47.6%, respectively, after 6 catalytic cycles. The decolorization capacity was reduced in the next catalytic cycles, but still occurred at a percentage of 38.1 and 32.9%, respectively, at the last catalytic cycle of usage. The results indicated that the immobilization of TvL on hybrid nanomaterials resulted in the formation of robust biocatalysts that were capable of repeatable use for the decolorization of synthetic dyes.

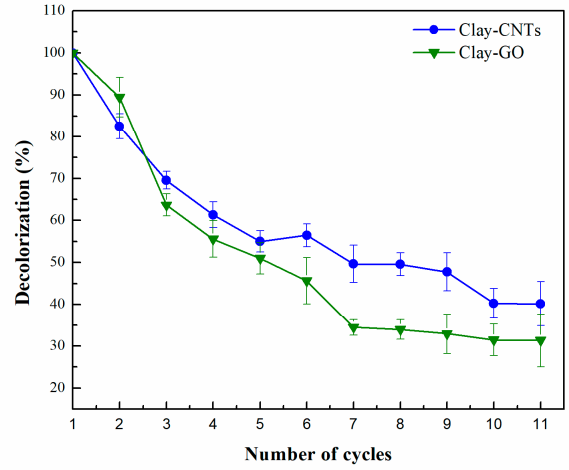


**Figure 3.** Reusability of covalently immobilized TvL on hybrid nanomaterials for the decolorization of methyl orange.

## 4. Conclusions

Herein, we demonstrated the synthesis of hybrid super-structures through the combination of carbon-based nanomaterials with smectite clays for the immobilization of TvL. The synthesized hybrid nanomaterials were found to be excellent supports for both non-covalent and covalent immobilization of TvL. The immobilization yield, as well as the catalytic activity of the immobilized enzyme, strongly depended on the nature of the nanomaterials, with covalently immobilized TvL on Clay-CNTs and Clay-GO to exhibit the highest apparent $V_{max}$ values amongst the nanobiocatalysts. In all cases, immobilized TvL exhibited higher thermal stability than the free enzyme, while FTIR analysis showed that the secondary structure of TvL remains unaltered upon immobilization, in most cases. The novel-synthesized nanobiocatalysts were used for the effective decolorization of a variety of synthetic dyes, presenting decolorization yields up to 91%, while they were able to catalyze the decolorization of methyl orange for up to 11 continuous reaction cycles with high efficiency. The results pronounce the use of these nanobiocatalytic systems in applications with environmental, biotechnological, and industrial interest.

**Supplementary Materials:** The following are available online at https://www.mdpi.com/article/10.3390/pr10020233/s1, Figure S1: FTIR spectra of (**a**) free TvL, (**b**) Clay-ADA nanomaterial and immobilized TvL on Clay-ADA, (**c**) Clay-CNTs nanomaterial and TvL immobilized on Clay-CNTs, (**d**) Clay-GO nanomaterial and immobilized TvL on Clay-GO, Figure S2: Decolorization of different dyes (75 μM) by (**a**) non-covalently and (**b**) covalently immobilized TvL on hybrid nanomaterials at 48 h. The reaction was conducted in acetate buffer (0.1 M, pH 4.58), at 30 °C, Figure S3: Effect of concentration of (**a**) bromophenol blue, (**b**) bromothymol blue, (**c**) Coomassie brilliant blue, (**d**) methyl orange, (**e**) phenol red, on the decolorization ability of covalently immobilized TvL on hybrid nanomaterials. The reaction was conducted in acetate buffer (0.1 M, pH 4.58), at 30 °C, for 48 h.

**Author Contributions:** Conceptualization, H.S.; methodology, M.P., P.E.A., L.K., G.P., A.K., D.G. and H.S.; software, M.P.; validation, M.P., L.K., G.P., A.K., D.G. and H.S.; investigation, M.P., P.E.A., G.P., A.K., D.G. and H.S.; resources, M.P., G.P., A.K., D.G. and H.S.; data curation, M.P.; writing—original draft preparation, M.P., G.P. and A.K.; writing—review and editing, D.G. and H.S.; visualization, M.P.; supervision, D.G. and H.S.; project administration, D.G. and H.S.; funding acquisition, H.S. All authors have read and agreed to the published version of the manuscript.

**Funding:** This work is co-financed by the European Union (European Regional Development Fund) and National Resources, under the operational program "Competitiveness, Entrepreneurship and Innovation (EPAnEK)", "NSRF 2014–2020", Call 111: "Support for Regional Excellence" (project: MIS 5047215).

**Institutional Review Board Statement:** Not applicable.

**Informed Consent Statement:** Not applicable.

**Data Availability Statement:** Not applicable.

**Conflicts of Interest:** The authors declare no conflict of interest.

## References

1. Moldes, D.; Fernández-Fernández, M.; Sanromán, M.Á. Role of laccase and low molecular weight metabolites from Trametes versicolor in dye decolorization. *Sci. World J.* **2012**, *2012*, 398725. [CrossRef] [PubMed]
2. Morsy, S.A.G.Z.; Ahmad Tajudin, A.; Ali, M.S.M.; Shariff, F.M. Current development in decolorization of synthetic Dyes by immobilized laccases. *Front. Microbiol.* **2020**, *11*, 1–8. [CrossRef] [PubMed]
3. Legerská, B.; Chmelová, D.; Ondrejovič, M. Degradation of synthetic dyes by laccases—A mini-review. *Nov. Biotechnol. Chim.* **2016**, *15*, 90–106. [CrossRef]
4. Rasheed, T.; Bilal, M.; Nabeel, F.; Adeel, M.; Iqbal, H.M.N. Environmentally-related contaminants of high concern: Potential sources and analytical modalities for detection, quantification, and treatment. *Environ. Int.* **2019**, *122*, 52–66. [CrossRef]
5. Sarkar, S.; Banerjee, A.; Halder, U.; Biswas, R. Degradation of synthetic azo dyes of textile industry: A sustainable approach using microbial enzymes. *Water Conserv. Sci. Eng.* **2017**, *2*, 121–131. [CrossRef]

6. Zhao, J.; Wu, Q.-X.; Cheng, X.-D.; Su, T.; Wang, X.-H.; Zhang, W.-N.; Lu, Y.-M. Biodegradation and detoxification of the triphenylmethane dye coomassie brilliant blue by the extracellular enzymes from mycelia of *Lactarius deliciosus*. *Front. Chem. Sci. Eng.* **2021**, *15*, 421–436. [CrossRef]
7. Telke, A.A.; Ghodake, G.S.; Kalyani, D.C.; Dhanve, R.S.; Govindwar, S.P. Biochemical characteristics of a textile dye degrading extracellular laccase from a *Bacillus* sp. ADR. *Bioresour. Technol.* **2011**, *102*, 1752–1756. [CrossRef]
8. Chatha, S.A.S.; Asgher, M.; Iqbal, H.M.N. Enzyme-based solutions for textile processing and dye contaminant biodegradation—A review. *Environ. Sci. Pollut. Res.* **2017**, *24*, 14005–14018. [CrossRef]
9. Chiong, T.; Lau, S.Y.; Hong, L.Z.; Koh, B.Y.; Danquah, M.K. Enzymatic treatment of methyl orange dye in synthetic wastewater by plant-based peroxidase enzymes. *J. Environ. Chem. Eng.* **2016**, *4*, 2500–2509. [CrossRef]
10. Abadulla, E.; Tzanov, T.; Costa, S.; Robra, K.-H.; Cavaco-Paulo, A.; Gübitz, G.M. Decolorization and detoxification of textile dyes with a laccase from *Trametes hirsuta*. *Appl. Environ. Microbiol.* **2000**, *66*, 3357–3362. [CrossRef]
11. Arregui, L.; Ayala, M.; Gómez-Gil, X.; Gutiérrez-Soto, G.; Hernández-Luna, C.E.; Herrera De Los Santos, M.; Levin, L.; Rojo-Domínguez, A.; Romero-Martínez, D.; Saparrat, M.C.N.; et al. Laccases: Structure, function, and potential application in water bioremediation. *Microb. Cell Fact.* **2019**, *18*, 1–33. [CrossRef] [PubMed]
12. Mayolo-Deloisa, K.; González-González, M.; Rito-Palomares, M. Laccases in food industry: Bioprocessing, potential industrial and biotechnological applications. *Front. Bioeng. Biotechnol.* **2020**, *8*, 1–8. [CrossRef] [PubMed]
13. Bassanini, I.; Ferrandi, E.E.; Riva, S.; Monti, D. Biocatalysis with laccases: An updated overview. *Catalysts* **2021**, *11*, 26. [CrossRef]
14. Dana, M.; Khaniki, G.B.; Mokhtarieh, A.A.; Davarpanah, S.J. Biotechnological and industrial applications of laccase: A review. *J. Appl. Biotechnol. Rep.* **2017**, *4*, 675–679.
15. Mate, D.M.; Alcalde, M. Laccase: A multi-purpose biocatalyst at the forefront of biotechnology. *Microb. Biotechnol.* **2017**, *10*, 1457–1467. [CrossRef]
16. Gkantzou, E.; Chatzikonstantinou, A.V.; Fotiadou, R.; Giannakopoulou, A.; Patila, M.; Stamatis, H. Trends in the development of innovative nanobiocatalysts and their application in biocatalytic transformations. *Biotechnol. Adv.* **2021**, *51*, 107738. [CrossRef]
17. Pavlidis, I.V.; Patila, M.; Bornscheuer, U.T.; Gournis, D.; Stamatis, H. Graphene-based nanobiocatalytic systems: Recent advances and future prospects. *Trends Biotechnol.* **2014**, *32*, 312–320. [CrossRef]
18. Patila, M.; Orfanakis, G.; Polydera, A.; Pavlidis, I.; Stamatis, H. Graphene-based nanobiocatalytic systems. In *Biocatalysis and Nanotechnology*; Grunwald, P., Ed.; Pan Stanford Pte. Ltd.: Singapore, 2017; pp. 243–277. ISBN 9781315196602.
19. Zhang, Y.; Wu, M.; Wu, M.; Zhu, J.; Zhang, X. Multifunctional carbon-based nanomaterials: Applications in biomolecular imaging and therapy. *ACS Omega* **2018**, *3*, 9126–9145. [CrossRef]
20. Patel, K.D.; Singh, R.K.; Kim, H.-W. Carbon-based nanomaterials as an emerging platform for theranostics. *Mater. Horiz.* **2019**, *6*, 434–469. [CrossRef]
21. Enotiadis, A.; Tsokaridou, M.; Chalmpes, N.; Sakavitsi, V.; Spyrou, K.; Gournis, D. Synthesis and characterization of porous clay-organic heterostructures. *J. Sol Gel Sci. Technol.* **2019**, *91*, 295–301. [CrossRef]
22. Chalmpes, N.; Kouloumpis, A.; Zygouri, P.; Karouta, N.; Spyrou, K.; Stathi, P.; Tsoufis, T.; Georgakilas, V.; Gournis, D.; Rudolf, P. Layer-by-Layer assembly of clay-carbon nanotube hybrid superstructures. *ACS Omega* **2019**, *4*, 18100–18107. [CrossRef] [PubMed]
23. Stathi, P.; Litina, K.; Gournis, D.; Giannopoulos, T.S.; Deligiannakis, Y. Physicochemical study of novel organoclays as heavy metal ion adsorbents for environmental remediation. *J. Colloid Interface Sci.* **2007**, *316*, 298–309. [CrossRef] [PubMed]
24. Nicotera, I.; Enotiadis, A.; Angjeli, K.; Coppola, L.; Gournis, D. Evaluation of smectite clays as nanofillers for the synthesis of nanocomposite polymer electrolytes for fuel cell applications. *Int. J. Hydrog. Energy* **2012**, *37*, 6236–6245. [CrossRef]
25. Spyrou, K.; Potsi, G.; Diamanti, E.K.; Ke, X.; Serestatidou, E.; Verginadis, I.I.; Velalopoulou, A.P.; Evangelou, A.M.; Deligiannakis, Y.; Van Tendeloo, G.; et al. Towards novel multifunctional pillared nanostructures: Effective intercalation of adamantylamine in graphene oxide and smectite clays. *Adv. Funct. Mater.* **2014**, *24*, 5841–5850. [CrossRef]
26. Pavlidis, I.V.; Tzialla, A.A.; Enotiadis, A.; Stamatis, H.; Gournis, D. Enzyme immobilization on layered and nanostructured materials. In *Biocatalysis in Polymer Chemistry*; Loos, K., Ed.; Copyright© 2011 Wiley-VCH Verlag GmbH & Co. KGaA: Weinheim, Germany, 2010; pp. 35–63. ISBN 9783527326181.
27. Cacciotti, I.; Lombardelli, C.; Benucci, I.; Esti, M. Clay/chitosan biocomposite systems as novel green carriers for covalent immobilization of food enzymes. *J. Mater. Res. Technol.* **2019**, *8*, 3644–3652. [CrossRef]
28. De Volder, M.F.L.; Tawfick, S.H.; Baughman, R.H.; Hart, A.J. Carbon nanotubes: Present and future commercial applications. *Science 80* **2013**, *339*, 535–539. [CrossRef]
29. Patila, M.; Chalmpes, N.; Dounousi, E.; Stamatis, H.; Gournis, D. Use of functionalized carbon nanotubes for the development of robust nanobiocatalysts. In *Methods in Enzymology*; Kumar, C.V., Ed.; Elsevier: Amsterdam, The Netherlands, 2020; Volume 630, pp. 263–301. ISBN 9780128201435.
30. Efthimiou, I.; Vlastos, D.; Ioannidou, C.; Tsilimigka, F.; Drosopoulou, E.; Mavragani-Tsipidou, P.; Potsi, G.; Gournis, D.; Antonopoulou, M. Assessment of the genotoxic potential of three novel composite nanomaterials using human lymphocytes and the fruit fly Drosophila melanogaster as model systems. *Chem. Eng. J. Adv.* **2021**, *9*, 100230. [CrossRef]
31. Gournis, D.; Karakassides, M.A.; Bakas, T.; Boukos, N.; Petridis, D. Catalytic synthesis of carbon nanotubes on clay minerals. *Carbon* **2002**, *40*, 2641–2646. [CrossRef]

32. Terzopoulou, Z.; Bikiaris, D.N.; Triantafyllidis, K.S.; Potsi, G.; Gournis, D.; Papageorgiou, G.Z.; Rudolf, P. Mechanical, thermal and decomposition behavior of poly(ε-caprolactone) nanocomposites with clay-supported carbon nanotube hybrids. *Thermochim. Acta* **2016**, *642*, 67–80. [CrossRef]
33. Simari, C.; Potsi, G.; Policicchio, A.; Perrotta, I.; Nicotera, I. Clay-carbon nanotubes hybrid materials for nanocomposite membranes: Advantages of branched structure for proton transport under low humidity conditions in PEMFCs. *J. Phys. Chem. C* **2016**, *120*, 2574–2584. [CrossRef]
34. Staudenmaier, L. Verfahren zur Darstellung der Graphitsäure. *Ber. Der Dtsch. Chem. Ges.* **1899**, *32*, 1394–1399. [CrossRef]
35. Stergiou, D.V.; Diamanti, E.K.; Gournis, D.; Prodromidis, M.I. Comparative study of different types of graphenes as electrocatalysts for ascorbic acid. *Electrochem. Commun.* **2010**, *12*, 1307–1309. [CrossRef]
36. Nethravathi, C.; Viswanath, B.; Shivakumara, C.; Mahadevaiah, N.; Rajamathi, M. The production of smectite clay/graphene composites through delamination and co-stacking. *Carbon* **2008**, *46*, 1773–1781. [CrossRef]
37. Bradford, M.M. A rapid and sensitive method for the quantitation of microgram quantities of protein utilizing the principle of protein-dye binding. *Anal. Biochem.* **1976**, *72*, 248–254. [CrossRef]
38. Tzialla, A.A.; Pavlidis, I.V.; Felicissimo, M.P.; Rudolf, P.; Gournis, D.; Stamatis, H. Lipase immobilization on smectite nanoclays: Characterization and application to the epoxidation of α-pinene. *Bioresour. Technol.* **2010**, *101*, 1587–1594. [CrossRef]
39. Fotiadou, R.; Patila, M.; Hammami, M.A.; Enotiadis, A.; Moschovas, D.; Tsirka, K.; Spyrou, K.; Giannelis, E.P.; Avgeropoulos, A.; Paipetis, A.; et al. Development of effective lipase-hybrid nanoflowers enriched with carbon and magnetic nanomaterials for biocatalytic transformations. *Nanomaterials* **2019**, *9*, 808. [CrossRef]
40. Wolfenden, B.S.; Willson, R.L. Radical-cations as reference chromogens in kinetic studies of one-electron transfer reactions: Pulse radiolysis studies of 2,2′-azinobis-(3-ethyl benzthiazoline-6-sulphonate). *J. Chem. Soc. Perkin Trans.* **1982**, *11*, 805–812. [CrossRef]
41. Jiang, D.S.; Long, S.Y.; Huang, J.; Xiao, H.Y.; Zhou, J.Y. Immobilization of Pycnoporus sanguineus laccase on magnetic chitosan microspheres. *Biochem. Eng. J.* **2005**, *25*, 15–23. [CrossRef]
42. Asgher, M.; Noreen, S.; Bilal, M. Enhancement of catalytic, reusability, and long-term stability features of Trametes versicolor IBL-04 laccase immobilized on different polymers. *Int. J. Biol. Macromol.* **2017**, *95*, 54–62. [CrossRef]
43. Patila, M.; Diamanti, E.K.; Bergouni, D.; Polydera, A.C.; Gournis, D.; Stamatis, H. Preparation and biochemical characterisation of nanoconjugates of functionalized carbon nanotubes and cytochrome c. *Nanomed. Res. J.* **2018**, *3*, 10–18. [CrossRef]
44. Tzialla, A.A.; Kalogeris, E.; Enotiadis, A.; Taha, A.A.; Gournis, D.; Stamatis, H. Effective immobilization of Candida antarctica lipase B in organic-modified clays: Application for the epoxidation of terpenes. *Mater. Sci. Eng. B Solid-State Mater. Adv. Technol.* **2009**, *165*, 173–177. [CrossRef]
45. Wang, Q.; Peng, L.; Li, G.; Zhang, P.; Li, D.; Huang, F.; Wei, Q. Activity of laccase immobilized on $TiO_2$-Montmorillonite Complexes. *Int. J. Mol. Sci.* **2013**, *14*, 12520–12532. [CrossRef] [PubMed]
46. Chatzikonstantinou, A.V.; Gkantzou, E.; Thomou, E.; Chalmpes, N.; Lyra, K.M.; Kontogianni, V.G.; Spyrou, K.; Patila, M.; Gournis, D.; Stamatis, H. Enzymatic conversion of oleuropein to hydroxytyrosol using immobilized β-glucosidase on porous carbon cuboids. *Nanomaterials* **2019**, *9*, 1166. [CrossRef] [PubMed]
47. Apriceno, A.; Bucci, R.; Girelli, A.M. Immobilization of laccase from *Trametes versicolor* on chitosan macrobeads for anthracene degradation. *Anal. Lett.* **2017**, *50*, 2308–2322. [CrossRef]
48. Lin, J.; Wen, Q.; Chen, S.; Le, X.; Zhou, X.; Huang, L. Synthesis of amine-functionalized $Fe_3O_4$@C nanoparticles for laccase immobilization. *Int. J. Biol. Macromol.* **2017**, *96*, 377–383. [CrossRef]
49. Dinçer, A.; Becerik, S.; Aydemir, T. Immobilization of tyrosinase on chitosan-clay composite beads. *Int. J. Biol. Macromol.* **2012**, *50*, 815–820. [CrossRef]
50. Benucci, I.; Liburdi, K.; Cacciotti, I.; Lombardelli, C.; Zappino, M.; Nanni, F.; Esti, M. Chitosan/clay nanocomposite films as supports for enzyme immobilization: An innovative green approach for winemaking applications. *Food Hydrocoll.* **2018**, *74*, 124–131. [CrossRef]
51. Asgher, M.; Noreen, S.; Bilal, M. Enhancing catalytic functionality of Trametes versicolor IBL-04 laccase by immobilization on chitosan microspheres. *Chem. Eng. Res. Des.* **2017**, *119*, 1–11. [CrossRef]
52. Patila, M.; Kouloumpis, A.; Gournis, D.; Rudolf, P.; Stamatis, H. Laccase-functionalized graphene oxide assemblies as efficient nanobiocatalysts for oxidation reactions. *Sensors* **2016**, *16*, 287. [CrossRef]
53. Patila, M.; Pavlidis, I.V.; Kouloumpis, A.; Dimos, K.; Spyrou, K.; Katapodis, P.; Gournis, D.; Stamatis, H. Graphene oxide derivatives with variable alkyl chain length and terminal functional groups as supports for stabilization of cytochrome c. *Int. J. Biol. Macromol.* **2016**, *84*, 227–235. [CrossRef]
54. Yang, X.Q.; Zhao, X.X.; Liu, C.Y.; Zheng, Y.; Qian, S.J. Decolorization of azo, triphenylmethane and anthraquinone dyes by a newly isolated *Trametes* sp. SQ01 and its laccase. *Process Biochem.* **2009**, *44*, 1185–1189. [CrossRef]
55. Othman, A.M.; González-Domínguez, E.; Sanromán, Á.; Correa-Duarte, M.; Moldes, D. Immobilization of laccase on functionalized multiwalled carbon nanotube membranes and application for dye decolorization. *RSC Adv.* **2016**, *6*, 114690–114697. [CrossRef]
56. Wen, X.; Zeng, Z.; Du, C.; Huang, D.; Zeng, G.; Xiao, R.; Lai, C.; Xu, P.; Zhang, C.; Wan, J.; et al. Immobilized laccase on bentonite-derived mesoporous materials for removal of tetracycline. *Chemosphere* **2019**, *222*, 865–871. [CrossRef] [PubMed]
57. Arabaci, G.; Usluoglu, A. The enzymatic decolorization of textile dyes by the immobilized polyphenol oxidase from quince leaves. *Sci. World J.* **2014**, *2014*, 685975. [CrossRef] [PubMed]

58. Teerapatsakul, C.; Parra, R.; Keshavarz, T.; Chitradon, L. Repeated batch for dye degradation in an airlift bioreactor by laccase entrapped in copper alginate. *Int. Biodeterior. Biodegrad.* **2017**, *120*, 52–57. [CrossRef]
59. Mogharabi, M.; Nassiri-Koopaei, N.; Bozorgi-Koushalshahi, M.; Nafissi-Varcheh, N.; Bagherzadeh, G.; Faramarzi, M.A. Immobilization of laccase in alginate-gelatin mixed gel and decolorization of synthetic dyes. *Bioinorg. Chem. Appl.* **2012**, *2012*, 823830. [CrossRef]
60. Patil, M.S.; Kapsikar, N.D.; Sardar, P.B. Decolorization of synthetic dyes by microbial crude laccase. *Biosci. Discov.* **2018**, *9*, 19–24. [CrossRef]
61. Antecka, K.; Zdarta, J.; Siwińska-Stefańska, K.; Sztuk, G.; Jankowska, E.; Oleskowicz-Popiel, P.; Jesionowski, T. Synergistic degradation of dye wastewaters using binary or ternary oxide systems with immobilized laccase. *Catalysts* **2018**, *8*, 402. [CrossRef]
62. Yamaguchi, H.; Honda, T.; Miyazaki, M. Application of enzyme-immobilization technique for microflow reactor. *J. Flow Chem.* **2016**, *6*, 13–17. [CrossRef]
63. Gkantzou, E.; Patila, M.; Stamatis, H. Magnetic microreactors with immobilized enzymes—From assemblage to contemporary applications. *Catalysts* **2018**, *8*, 282. [CrossRef]